Langmuir
Article
pubs.acs.org/Langmuir

Manipulating Protein Adsorption using a Patchy Protein-Resistant Brush

Saugata Gon,[†] Marina Bendersky,[†] Jennifer L. Ross,[‡] and Maria M. Santore*[,§]

[†]*Department of Chemical Engineering,* [‡]*Department of Physics, and* [§]*Department of Polymer Science and Engineering, University of Massachusetts, Amherst, Massachusetts 01003*

Received April 26, 2010

Toward the development of surfaces for the precise manipulation of proteins, this study explores the fabrication and protein-interactive behavior of a new type of surface containing extremely small (on the order of 10 nm or less) flat adhesive "patches" or islands embedded in and partially concealed by a protein-repellant PEG (poly(ethylene glycol)) brush. The adsorption of fibrinogen, the model protein chosen to probe the biomaterial interactions of these surfaces, is very sensitive to the surface density of the adhesive patches, occurring only above a threshold. This suggests that two or more adhesive patches are needed to capture each protein. When the average spacing of the adhesive patches exceeds the fibrinogen length, no adsorption occurs because individual patches are too weakly binding for protein capture, as a result of being at least partially obstructed by the brush. The small size of the adhesive patches relative to the 47 nm fibrinogen length thus defines a limiting regime of surface design, distinct from surfaces where larger features can adhere single isolated proteins or multiple proteins together. The restricted protein−surface contact may comprise a means of preserving protein structure and function in the adsorbed state. This article demonstrates several additional interesting features of PEG brushes relevant to biomaterial design. First a moderate amount of adhesive material can be buried at the base of a brush without a measurable impact on the corona density. Second, a different amount of material at the base of a brush can be rendered ineffective to capturing adhesive proteins, despite a modest compromise of the brush corona. From this will follow insight into the design of patterned biomaterial surfaces, the bioactivity of the edges of patterned features, and an understanding of how flaws in brushes compromise protein resistance or allow access to small adhesive sites.

Introduction

The design of surfaces for the control of protein adsorption has been a scientific and industrial endeavor for the past several decades, with the goals ranging from complete avoidance of protein adsorption (and cell adhesion) for some implants to selective reversible protein binding for pharmaceutical separations and addressable specific targeting elements in protein chip arrays and diagnostics. Common strategies include the immobilization of biospecific ("affinity") capture molecules and the passivation of the remaining surface. Often, lithographic methods enable the controlled placement of adhesive and nonadhesive moieties, enabling addressability. Typically, pattern length scales have exceeded protein dimensions so that multiple proteins adhere to each adhesive region. This is an advantage in many applications, for instance, when multiple bound proteins produce a strong signal; however, one can envision situations in which it is desirable to adhere single isolated proteins or a few clustered target proteins. Here adhesive surface regions need to be just a few nanometers. Advances in lithography are bringing nanoscopic length scales within reach, at least for small-scale production. Lagging behind, however, is a larger-scale means to produce surfaces with nanoscale protein-adhesive features. Also lagging behind is a fundamental understanding of interfacial protein behavior when interfacial length scales and patterns approach and become smaller than the dimensions of the proteins themselves.

Many proteins spread and denature substantially on large areas of adhesive surfaces.[1−8] It follows, then, that limiting protein−surface contact is a potential means of achieving protein adhesion without denaturing. This challenge, however, requires the fine tuning of binding energies and contact areas to ensure protein retention while avoiding unfolding. Steps have been taken in this direction employing nanoparticles.[9−12] For instance, it has been reported that albumin is more stable to denaturing when adsorbed onto small rather than large gold nanoparticles.[13] Related to these findings and providing further motivation for the immobilization of small numbers of proteins is the observation that the edges of a 2D lysozyme pattern are more accessible to antibody binding than the proteins in the main area of the pattern.[14]

The current study develops patchy polymer brushes as a means of controlling adhesive protein contact. By way of background, hydrated polymer brushes such as PEG (poly(ethylene glycol))[15−19]

(1) Chang, B. S.; Kendrick, B. S.; Carpenter, J. F. *J. Pharm. Sci.* **1996**, *85*, 1325–1330.
(2) Bos, M. A.; van Vliet, T. *Adv. Colloid Interface Sci.* **2001**, *91*, 437–471.
(3) Agnihotri, A.; Siedlecki, C. A. *Langmuir* **2004**, *20*, 8846–8852.
(4) Dickinson, E. *Colloids Surf., B* **1999**, *15*, 161–176.
(5) Haynes, C. A.; Norde, W. *J. Colloid Interface Sci.* **1995**, *169*, 313–328.
(6) Norde, W. *Cells Mater.* **1995**, *5*, 97–112.
(7) Wertz, C. F.; Santore, M. M. *Langmuir* **2002**, *18*, 706–715.
(8) Santore, M. M.; Wertz, C. F. *Langmuir* **2005**, *21*, 10172–10178.
(9) Billsten, P.; Wahlgren, M.; Arnebrant, T.; McGuire, J.; Elwing, H. *J. Colloid Interface Sci.* **1995**, *175*, 77–82.
(10) Cedervall, T.; Lynch, I.; Lindman, S.; Berggard, T.; Thulin, E.; Nilsson, H.; Dawson, K. A.; Linse, S. *Proc. Natl. Acad. Sci. U.S.A.* **2007**, *104*, 2050–2055.
(11) Karajanagi, S. S.; Vertegel, A. A.; Kane, R. S.; Dordick, J. S. *Langmuir* **2004**, *20*, 11594–11599.
(12) Shang, L.; Wang, Y. Z.; Jiang, J. G.; Dong, S. J. *Langmuir* **2007**, *23*, 2714–2721.
(13) Teichroeb, J. H.; Forrest, J. A.; Jones, L. W. *Eur. Phys. J. E* **2008**, *26*, 411–415.
(14) Gao, P.; Cai, Y. G. *Langmuir* **2008**, *24*, 10334–10339.
(15) Kenausis, G. L.; Voros, J.; Elbert, D. L.; Huang, N. P.; Hofer, R.; Ruiz-Taylor, L.; Textor, M.; Hubbell, J. A.; Spencer, N. D. *J. Phys. Chem. B* **2000**, *104*, 3298–3309.
(16) McPherson, T.; Kidane, A.; Szleifer, I.; Park, K. *Langmuir* **1998**, *14*, 176–186.
(17) Sofia, S. J.; Premnath, V.; Merrill, E. W. *Macromolecules* **1998**, *31*, 5059–5070.
(18) Mrksich, M.; Chen, C. S.; Xia, Y. N.; Dike, L. E.; Ingber, D. E.; Whitesides, G. M. *Proc. Natl. Acad. Sci. U.S.A.* **1996**, *93*, 10775–10778.
(19) Stolnik, S.; Illum, L.; Davis, S. S. *Adv. Drug Delivery Rev.* **1995**, *16*, 195–214.

 DOI: 10.1021/la1016752

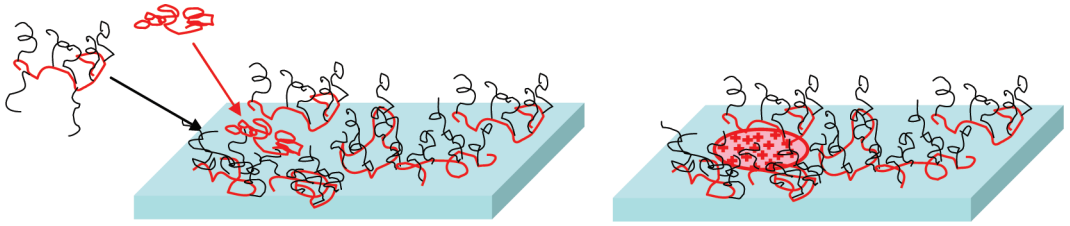

Figure 1. Protein-resistant brush with a flat embedded adhesive cationic patch. In the more realistic schematic on the left, the cationic patch is difficult to see. The cartoon patch on the right highlights the region of the surface in which the cationic chain is not connected to PEG tethers.

or certain zwitterionic polymers[20,21] have, when end-tethered on surfaces with an appropriate density and molecular weight, proven to eliminate protein adsorption almost entirely. By strict definition in the polymer physics community, a "brush" is produced when polymer chains are end-grafted to an interface in a good solvent, with the grafting spacing smaller than the characteristic free coil size by about an order of magnitude.[22−24] As a result of the osmotic pressure generated by the good solvent, segmental repulsions stretch the polymer chain normal to the interface and can prevent the close approach of proteins or other brushy objects. It is noted, however, that in most cases of bioinertness and near-perfect protein repellency, the brush density and height fall substantially short of the rigorous definition.[25−28] Thus it is the case, especially in the biomaterial community, that the term brush is used loosely, as we do here. (Indeed, until the advent of surface-initiated polymerization, the adsorption method of depositing brushes always fell short of the coverages of a true brush.[28] However, adsorption continues to be the preferred method of brush placement because of its economic and processing advantages.)

This article explores the use of patchy brushes as materials for the manipulation of protein adsorption and potentially for protein separation or biomaterial applications. These surfaces contain relatively flat nanoscale adhesive regions surrounded by a polymer protein-resistant polymer brush, shown schematically in Figure 1. Although the adhesive elements or patches could have any arbitrary chemistry, here they are cationic. The current patchy brushes are modeled after the electrostatically patchy surfaces that we previously studied in detail,[29−31] but the current surfaces employ brushes on the main surface region as opposed to the negative charge of the prior body of work. The size of the adhesive regions, 10 nm or less, is small relative to the protein size, limiting protein contact with the surface.

This article reports the interaction of these patchy brush surfaces with fibrinogen, which was chosen because of its importance in different applications and its tendency to adhere to many different surface types. This is a result of its substantial hydrophobicity and electrostatic heterogeneity: Fibrinogen's central e domain is positively charged, but the protein charge is overall net negative.[32] Although fibrinogen is relatively large, roughly 47 × 4.5 × 4.5 nm^3,[33] it has been shown to adhere to relatively small surface features, for instance, the interstices of a saturated adsorbed albumin layer (i.e., after no further albumin would adhere[34]).

This article demonstrates a simple method for the creation of patchy brushes and reports their basic behavior in terms of protein interactions. Here we demonstrate that patches can be made sufficiently small/weakly binding that single patches are not able to adsorb protein. When the surface density of the patches becomes sufficiently high that fibrinogen can interact with multiple patches at once, limited adsorption occurs. The work demonstrates how flaws or contaminants can be accommodated in a polymer brush without altering its structure and then goes on to demonstrate how these flaws or adhesive regions potentially lead to bioadhesion.

Materials and Methods

Poly-L-lysine hydrobromide (PLL) with a nominal molecular weight of 20 000 was purchased from Sigma-Aldrich and was used for the cationic patches and as the anchoring component of the PEG brush. The PEG brush was formed by the adsorption of a graft copolymer consisting of a PLL backbone and PEG side chains, with the latter having a nominal molecular weight of 2300 g/mol. The use of PLL-PEG bottle-brush graft copolymers as protein-resistant coatings was developed by Hubbell and Textor[15,35] and extensively studied by those groups.[36−40] Our synthesis of PLL-PEG follows their procedure,[15,35] and indeed, we employed copolymer compositions near their reported optimum for protein resistance, that is, copolymers having a grafting ratio between 2.8 and 3.0. The grafting ratio is the number of PLL monomers divided by the number of PEG chains.

To synthesize the PLL-PEG copolymers, PLL was dissolved in 50 mM pH 9.1 sodium borate buffer. The *N*-hydroxysuccinimidyl ester of methoxypoly(ethylene glycol) acetic acid (Laysan Bio Inc.) was added, and the solution was stirred for 6 h and then dialyzed against pH 7.4 phosphate-buffered saline for 24 h. It then was further dialyzed against DI water for another 24 h. The final product was freeze dried and stored at −20 °C.

(20) Ladd, J.; Zhang, Z.; Chen, S.; Hower, J. C.; Jiang, S. *Biomacromolecules* **2008**, *9*, 1357–1361.
(21) Chen, S. F.; Zheng, J.; Li, L. Y.; Jiang, S. Y. *J. Am. Chem. Soc.* **2005**, *127*, 14473–14478.
(22) Milner, S. T. *Science* **1991**, *251*, 905–914.
(23) de Gennes, P. G. *J. Phys.* **1976**, *38*, 1443.
(24) Alexander, S. *J. Phys.* **1977**, *38*, 977.
(25) Dalsin, J. L.; Lin, L. J.; Tosatti, S.; Voros, J.; Textor, M.; Messersmith, P. B. *Langmuir* **2005**, *21*, 640–646.
(26) Dalsin, J. L.; Hu, B. H.; Lee, B. P.; Messersmith, P. B. *J. Am. Chem. Soc.* **2003**, *125*, 4253–4258.
(27) Kent, M. S.; Lee, L. T.; Factor, B. J.; Rondelez, F.; Smith, G. S. *J. Chem. Phys.* **1995**, *103*, 2320–2342.
(28) Brittain, W. J.; Minko, S. *J. Polym. Sci., Part A: Polym. Chem.* **2007**, *45*, 3505–3512.
(29) Kozlova, N.; Santore, M. M. *Langmuir* **2006**, *22*, 1135–1142.
(30) Kalasin, S.; Santore, M. M. *Langmuir* **2008**, *24*, 4435–4438.
(31) Duffadar, R. D.; Kalasin, S.; Davis, J. M.; Santore, M. M. *J. Colloid Interface Sci.* **2009**, *337*, 396−407.
(32) Feng, L.; Andrade, J. D. In *Proteins at Interfaces II: Fundamentals and Applications*; Horbett, T. A., Brash, J. L., Eds.; American Chemical Society: Washington, DC, 1994; Vol. *602*, pp 66−79.
(33) Toscano, A.; Santore, M. M. *Langmuir* **2006**, *22*, 2588–2597.
(34) Wertz, C. F.; Santore, M. M. *Langmuir* **1999**, *15*, 8884–8894.
(35) Huang, N. P.; Michel, R.; Voros, J.; Textor, M.; Hofer, R.; Rossi, A.; Elbert, D. L.; Hubbell, J. A.; Spencer, N. D. *Langmuir* **2001**, *17*, 489–498.
(36) Tosatti, S.; Schwartz, Z.; Campbell, C.; Cochran, D. L.; VandeVondele, S.; Hubbell, J. A.; Denzer, A.; Simpson, J.; Wieland, M.; Lohmann, C. H.; Textor, M.; Boyan, B. D. *J. Biomed. Mater. Res.* **2004**, *68A*, 458–472.
(37) Pasche, S.; De Paul, S. M.; Voros, J.; Spencer, N. D.; Textor, M. *Langmuir* **2003**, *19*, 9216–9225.
(38) Tosatti, S.; De Paul, S. M.; Askendal, A.; VandeVondele, S.; Hubbell, J. A.; Tengvall, P.; Textor, M. *Biomaterials* **2003**, *24*, 4949–4958.
(39) VandeVondele, S.; Voros, J.; Hubbell, J. A. *Biotechnol. Bioeng.* **2003**, *82*, 784–790.
(40) Huang, N. P.; Voros, J.; De Paul, S. M.; Textor, M.; Spencer, N. D. *Langmuir* **2002**, *18*, 220–230.

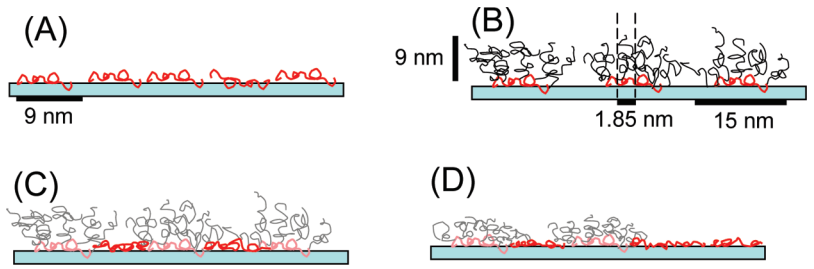

Figure 2. Features of interfacial components. (A) Saturated PLL layer showing the diameter of the excluded footprint. (B) Saturated PLL-PEG layer showing the diameter of the excluded footprint of the PLL-PEG copolymer and the effective diameter for a single anchored PEG chain (tether). (C) Inclusion of PLL patches at the base of a brush without reducing the tether (PLL-PEG) density. Here the graft copolymers are drawn in pale ink to emphasize the PLL patches. (D) Greater PLL loading reduces PLL-PEG coverage, thus reducing crowding and ultimately PEG chain stretching.

PLL-PEG was characterized with ^{1}H NMR using a D_2O solvent with a Bruker 400 MHz instrument. The areas of the lysine side-chain peak ($-CH_2-N-$) at 2.909 ppm and the PEG peak ($-CH_2-CH_2-$) at 3.615 ppm were compared to determine the grafting ratio.

Bovine serum fibrinogen (fraction I, type 1-s) was purchased from Sigma (F8630-1G). In the runs in the published Figures, which employed optical reflectometry, the protein was used as received. Control and calibration studies (which are key to the work but are not shown in the Figures) employed fluorescein-tagged fibrinogen in a total internal reflectance fluorescence apparatus. The labeling was conducted as previously described, and purification was accomplished by passing the protein solution through a P-6 gel column.[34]

The adsorption substrates for this study were acid-etched microscope slides. In our procedure, overnight soaking in concentrated sulfuric acid followed by copious rinsing in DI (deionized water) leaches metal ions from the soda−lime glass to produce a pure silica surface, as characterized by XPS.[33]

Polymer and protein adsorption were conducted in a laminar slit shear flow cell[41] with a wall shear rate of 5 s^{-1} using polymers dissolved in 0.01 M pH 7.4 phosphate buffer. In the main portion of the study, adsorption was monitored with near-Brewster optical reflectometry, a method that is sensitive to the refractive index of the layer and requires no labeling of the adsorbing molecules. In our instrument,[42] a parallel-polarized HeNe laser impinges on the liquid−solid interface from the solid side. Near the Brewster condition, the back reflected beam is vanishingly small, arising primarily from the etched silica layer on the microscope slide. As adsorption proceeds, however, the intensity grows in a fashion that can be adequately quantified using a step profile optical model. For the different interfacial layers (polymer and protein) in the current study, the overall mass is sufficiently small that this treatment works well, though different refractive indices potentially apply to the polymer and protein layers.[42]

Control runs were performed using total internal reflectance fluorescence with the same flow chamber.[43] By labeling either the PLL or the fibrinogen with fluorescein or rhodamine-*b*-isothiocyanate[34] (ITC), we were able to prove the additivity of the different portions of the reflectometry runs. TIRF was also employed to establish that PLL and PLL-PEG molecules were not displaced during fibrinogen adsorption. A rhodamine-*b*-ITC-labeled PLL sample was employed in single fluorohpore imaging studies of the distribution of PLL chains on the surface.

Total internal reflection fluorescence imaging of polymer-coated surfaces was performed with a home-built laser system (488 and 532 nm) built around a Nikon Ti-E inverted microscope using through-the-lens illumination (60× objective, NA 1.49). Images were recorded on a Cascade (Roper Scientific) electron-multiplier CCD camera with a 1 s exposure time using an EM gain set at 3564. Data was analyzed with ImageJ by selecting individual particles after establishing a threshold and measuring the intensity.

Zeta potentials for saturated layers of PLL and PLL-PEG on silica were determined using 1 μm silica spheres from GelTech (Orlando, FL), onto which varying amounts of these polymer had been adsorbed. The ionic strength conditions for adsorption and zeta potential measurement corresponded to those used in the corresponding portions of the main study. A Malvern Zeta Sizer Nano ZS instrument was employed.

Table 1. Properties of Saturated PLL and PLL-PEG Layers

	PLL	PLL-PEG
nominal molecular weight, g/mol	20 000	147 100
free solution hydrodynamic diameter, nm	7 nm	
saturated layer covg, mg/m^2	0.4 ± 0.02	1.1 ± 0.1
effective chain footprint, nm^2 (= MW/Γ sat)	83 ± 10	220 ± 22
zeta potential of the saturated layer, mV	+5 mV	−15 mV

Results

Features of Patchy Brush Surfaces. Some properties of the patchy brush surfaces can be deduced from the interfacial properties of the component polymers, which are summarized in Table 1.

PLL Patches. We first discuss features of the PLL patches that can be inferred from the properties of PLL layers (Figure 2A). In Table 1, PLL having a nominal molecular weight of 20 000 forms saturated layers with a coverage of 0.4 mg/m^2, which is typical of other densely charged cationic polymers on silica at pH 7.4.[44] Coverage is independent of free solution concentration over a large range, as a result of the substantial segment−surface binding energy. In general, when densely charged cationic polymers adsorb on a negative substrate, the backbone lies flat against the surface.[45,46] This is particularly true at coverages well below saturation, which is pertinent to the current isolated cationic patches. Consistent with this scenario is the mildly positive zeta potential of saturated PLL layers on silica. The mild overcompensation of charge by saturated PLL layers suggests that isolated PLL chains adsorbed at low coverage will also be locally positively charged. Patches can also be expected to be relatively flat.[29]

The net positive charge on the PLL chains gives rise to modest patch−patch repulsions on the surface that limit the ultimate PLL coverage. Near neutral pH when the ionic strength is raised from 0.01 to 0.1 M, the PLL coverage increases by about 20%.[47] This is

(41) Shibata, C. T.; Lenhoff, A. M. *J. Colloid Interface Sci.* **1992**, *148*, 485–507.
(42) Fu, Z. G.; Santore, M. M. *Colloids Surf., A* **1998**, *135*, 63–75.
(43) Rebar, V. A.; Santore, M. M. *Macromolecules* **1996**, *29*, 6262–6272.
(44) Hansupalak, N.; Santore, M. M. *Langmuir* **2003**, *19*, 7423–7426.
(45) Shin, Y.; Roberts, J. E.; Santore, M. M. *Macromolecules* **2002**, *35*, 4090–4095.
(46) Fleer, G. J.; Cohen Stuart, M. A.; Scheutjens, J. M. H. M.; Cosgrove, T.; Vincent, B. In *Polymers at Interfaces*; Chapman and Hall: London: 1993, p2993.
(47) Jiang, M.; Popa, I.; Maroni, P.; Borkovec, M. *Colloids Surf., A* **2010**, *360*, 20–25.

 DOI: 10.1021/la1016752 C

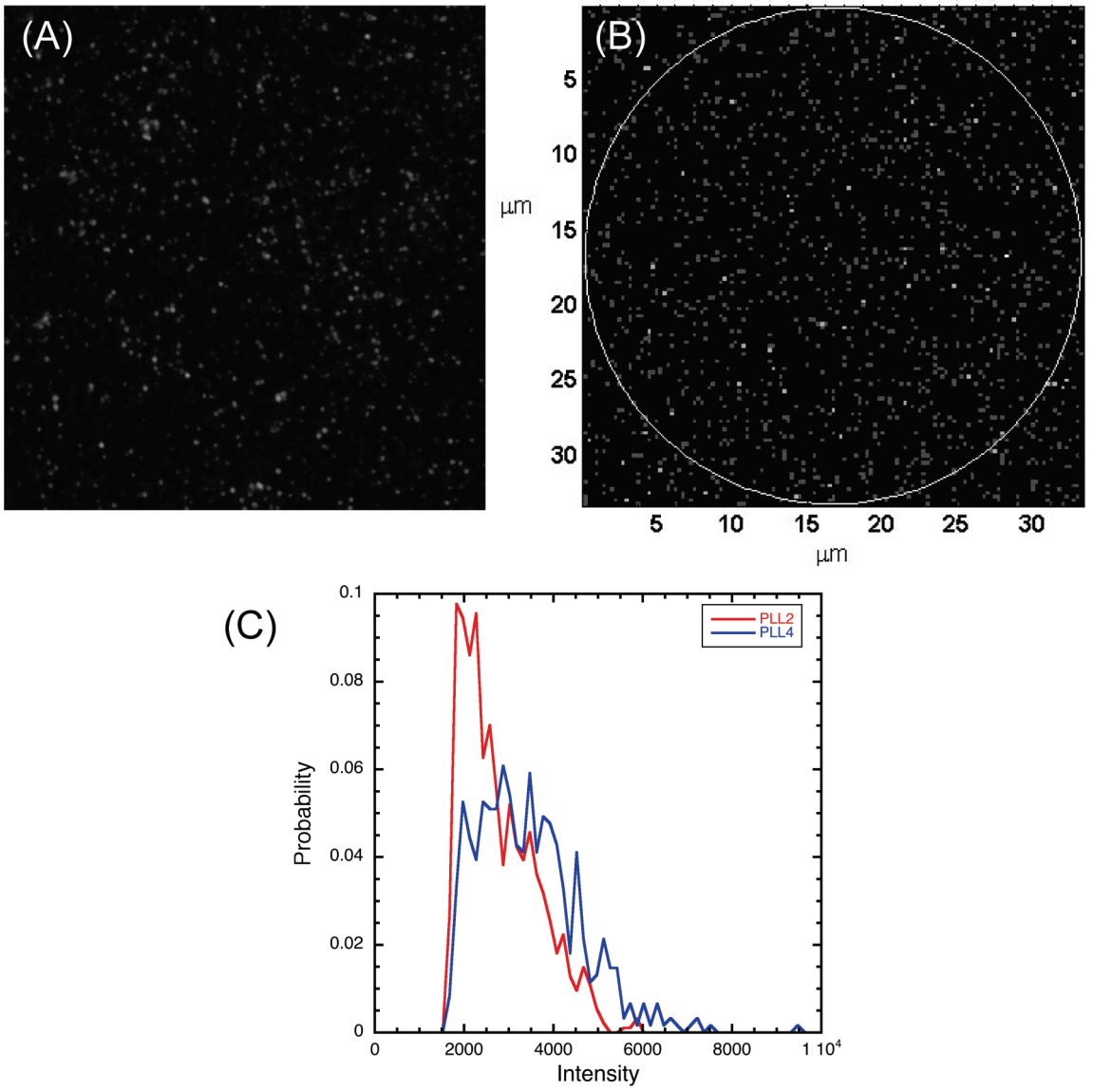

Figure 3. (A) Micrograph (33×33 μm^2) containing roughly 500 PLL/μm^2, a trace amount of which is fluorescently labeled to give 1.5 fluorophores/μm^2 corresponding to 1500 illuminated spots, some of which may overlap. (B) Image simulated in Matlab with 1500 spots distributed randomly over the same area. Here, doubles are brighter. (C) Distribution of spot intensities for two surfaces like those in part A with 1.5 and 3 labels per μm^2.

consistent with the reduction of the Debye length from 3 to just under 1 nm. With the 2 nm Debye length under conditions for our patch deposition (ionic strength $I = 0.026$ M for a phosphate buffer concentration of 0.01 M), no patch ordering or other special long-range effects of patch−patch interactions are expected in our studies. It is worth noting, however, that the documented presence of repulsions between adsorbing PLL chains and the impact of these repulsions on the PLL adsorption on silica argue against any PLL surface aggregation.

One metric of the patch size of adsorbed PLL is derived from its free solution hydrodynamic coil diameter, $d_h = 7$ nm, from dynamic light scattering. A second measure of the adsorbed coil size is derived from the excluded footprint of a chain in a saturated PLL layer. Dividing the molecular weight by the adsorbed amount in a saturated layer and converting units reveals a footprint of 83 nm^2, giving a diameter (of "gyration", a statistical measure) of $d_g = 9.1$ nm. The free solution hydrodynamic diameter is consistent with this value because it is generally accepted that polyelectrolytes at moderate and high ionic strengths act like neutral chains. Then, a nondraining model relates the hydrodynamic to the statistical size: $d_h = 0.676 d_g$.[48]

As demonstrated previously with other systems[29,33,49] and in the Supporting Information for PLL, using a shear flow cell with well-characterized mass transport, we are able to deposit PLL in controlled amounts down to extremely low coverage, where individual coils are randomly isolated on the surface. Our previous study of pDMAMEA (poly(dimethylaminoethyl methacrylate)) polycation adsorption has demonstrated the nearly random arrangement of polycations adsorbed in this fashion on silica, especially in the dilute range of patch loading relevant to the current work.[31] Additionally, we have found that the tight binding of polycations on a negative surface prevents chain translation along the surface that would tend to reduce order.

The random distribution of the adsorbed patches is further strongly supported in Figure 3. Figure 3A shows a micrograph of

(48) Yamakawa, H. In *Modern Theory of Polymer Solutions*; Harper and Row: New York, 1971.
(49) Zhang, J.; Srivastava, S.; Duffadar, R.; Davis, J. M.; Rotello, V. M.; Santore, M. M. *Langmuir* **2008**, *24*, 6404–6408.

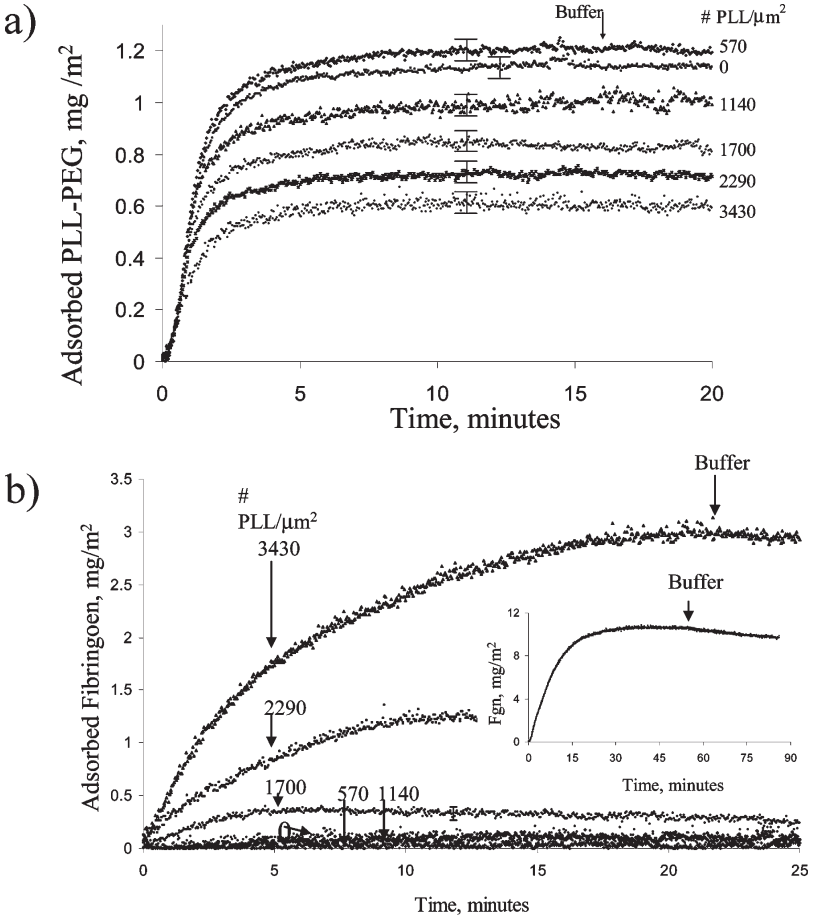

Figure 4. (a) PLL-PEG adsorption following different coverages of preadsorbed PLL, where the PLL coverage level is indicated but the adsorption traces are not shown. (b) Fibrinogen adsorption onto patchy brushes having different PLL patch densities as indicated. Only fibrinogen adsorption is shown, with PLL and PLL-PEG adsorption measured prior to this point in each run. The inset shows fibrinogen adsorption on a saturated PLL layer (containing no PLL-PEG).

a patchy PLL layer containing 500 chains/μm^2 as established by the controlled deposition demonstrated in the Supporting Information. In fabricating this specimen, a PLL sample containing an average of 0.6 rhodamine tags per PLL chain was diluted into an unlabeled PLL solution and exposed via steady flow to the substrate under tightly controlled timing to produce a surface having 1.5 rhodamine tags/μm^2 with 500 PLL chains total/μm^2. The intent of this surface composition was to produce an image containing diffraction-limited spots for the individual fluorophores. (One fluorophore on each of 500 chains/μm^2 would have produced a layer too densely labeled to resolve individual labels.) Given the scale of the micrograph, one expects roughly 1500 fluorophores in the image. Several spots (1300) are actually counted, indicating that some of the diffraction-limited spots, each 250 nm in diameter, contain 2 or more fluorophores, as expected for a random distribution (and for the finite probability of 2 labels on some of the chains). Indeed, Figure 3B shows that a simulated image of randomly positioned spots in the same field is similar in randomness to the micrograph, confirming the overall random distribution of our patches and a lack of PLL aggregation on the surface. Figure 3C addresses the fact that fewer than 1% of the chains in Figure 3A carry fluorescent labels. Here the distribution of intensity per spot indicates that some spots contain multiple fluorophores. As the amount of fluorescent PLL is increased while keeping the total PLL patch loading constant, the distribution shifts proportionally to the right, indicating a greater incidence of spots with multiple fluorophores.

In summary, the features of saturated PLL layers along with other data suggest that when individual PLL chains are sparsely adsorbed on silica the resulting patches are about 9 nm in size, lie flat on the surface, are randomly arranged, and locally present a positive charge. Data in the Supporting Information demonstrates that the patches resist desorption in pH 7.4 buffer and withstand challenges by PLL-PEG and fibrinogen. Prior work suggests that they do not diffuse laterally on the surface on timescales relevant to our study.[29,50,51]

PLL-PEG Brushes. The saturation coverage of 1.1 ± 0.1 mg/m^2 for PLL-PEG on bare silica (in Table 1 and Figure 4) provides quantitative insight into the features of the PEG brush: With a grafting ratio of 2.8 and a PEG molecular weight of 2000, this saturation coverage corresponds to 220 ± 20 nm^2 per adsorbed PLL-PEG molecule and 3.4 nm^2 per interfacial PEG chain, or a 1.85-nm-diameter footprint for a tether. These dimensions are shown schematically in Figure 2B. The calculated unperturbed (θ solvent) end−end distance of a 2000 molecular weight PEG chain is 3.35 nm (radius = 1.67 nm), or, with the classic $^3/_5$ power law scaling of molecular weight expected in a good solvent, the maximum coil radius might be as large as 2.4 nm. Therefore, the PEG chains tethered to our surfaces by PLL anchors are sufficiently closely tethered to be forced to stretch normal to the surface. A brush height of 9 nm is estimated in the Supporting Information.

(50) Santore, M. M. *Curr. Opin. Colloid Interface Sci.* **2005**, *10*, 176–183.
(51) Hansupalak, N.; Santore, M. M. *Macromolecules* **2004**, *37*, 1621–1629.

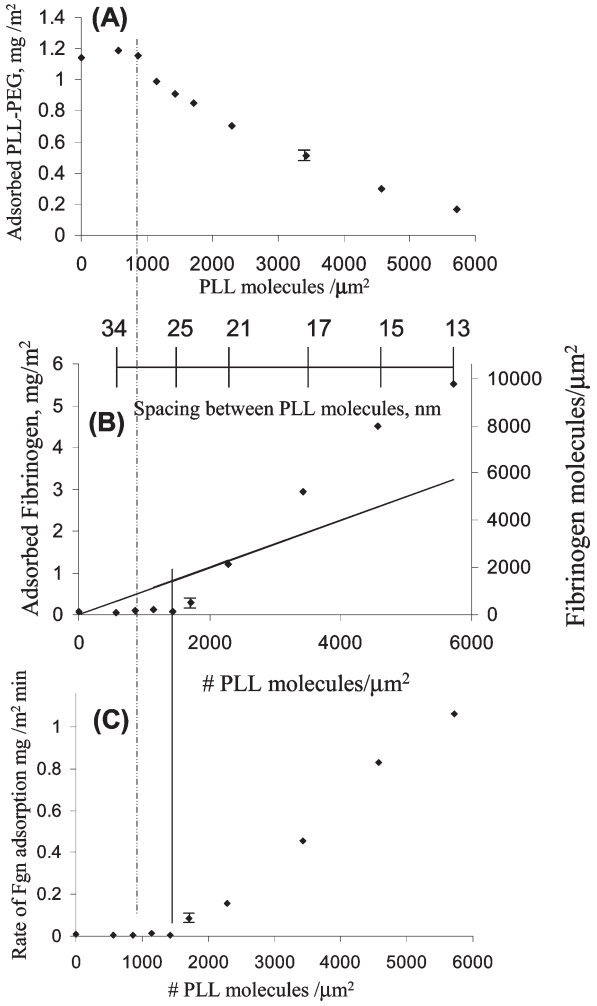

Figure 5. Summary of the impact of PLL patch density on (A) the amount of PLL-PEG backfill (B) short-term fibrinogen coverage, and (C) the initial fibrinogen adsorption rate.

The larger excluded footprint (220 nm^2) of chains within a pure saturated PLL-PEG layer compared with those within a pure saturated PLL layer (83 nm^2) in Table 1 is significant. This difference indicates that in the PLL-PEG layer it is the PEG rather than the PLL backbone that limits the brush coverage. The lower content of PLL backbones within the PLL-PEG layer, per Figure 2A,B, is also consistent with the negative zeta potential of the saturated PLL-PEG surfaces.

Patchy Brushes. Patchy brushes were created by first depositing controlled amounts of PLL from dilute flowing solution (as shown in the Supporting Information) and, following a buffer rinse, backfilling with PLL-PEG. (Control studies using fluorescently labeled PLL have demonstrated the full retention of the PLL patches throughout this process.) Figure 4 presents reflectometry data for the PLL-PEG backfilling portion of the process for surfaces containing different densities of preadsorbed PLL patches. With no PLL preadsorbed, the saturation coverage for PLL-PEG on bare silica is 1.1 ± 0.1 mg/m^2 and its initial adsorption onto silica is transport-limited. As the amount of preadsorbed PLL is increased, the ultimate PLL-PEG coverage decreases; however, the adsorption kinetics are mostly unaffected. The flat signal following buffer reinjection demonstrates the stability of the composite layers at these conditions.

Figure 5A summarizes the data in Figure 4 by plotting the amount of PLL-PEG backfill as a function of the initially adsorbed PLL patch density. This representation demonstrates that small amounts of PLL, below 900 chains/μm^2, can be accommodated at the interface without reducing the overall brush density, as shown schematically in Figure 2C. The mechanism derives from the smaller excluded footprint of PLL compared with PLL-PEG in pure saturated layers, in Table 1 and Figure 2A-B. The lower backbone content of the saturated PLL-PEG layers, compared with a saturated layer of pure PLL provides an opportunity for limited PLL incorporation at the base of the brush. At the point where the maximum amount of PLL chains have been incorporated into the base of the brush, there are about 5400 PLL chains/μm^2 on the surface, either as part of the PLL-PEG chains (4500/μm^2) or as PLL patches (900/μm^2). This is far less than the 12,000 PLL chains/μm^2 in a pure saturated PLL layer. The difference provides evidence for the lack of mobility of the adsorbed chains. Were chains sufficiently mobile on the surface, they might rearrange to accommodate a greater density of PLL at the base of the brush.

When PLL patch densities exceed 0.03 mg/m^2 (900 chains/μm^2), additional PLL patches reduce the amount of PLL-PEG needed for backfilling. Over most of this regime, each PLL patch added to the surface reduces the PLL-PEG backfill by one chain. (We note, however, that the decay has some curvature, so the effective chain exchange percentage is initially higher. Our point here is that the displacement occurs near the order of 1−1 chain swapping.) Ultimately, a saturated layer of PLL completely excludes PLL-PEG. As the number of PEG tethers decreases with an increasing number of PLL patches, the overall average quality of the brush is reduced (i.e., the average chain becomes less extended normal to the surface because the tethers are progressively less crowded) (Figure 2D).

Fibrinogen Adsorption on Patchy Surfaces. For each run in Figure 4A, after PLL-PEG backfilling and exposure to flowing buffer for several minutes, the surfaces were exposed to 100 ppm solutions of flowing fibrinogen, with the resulting kinetic traces in Figure 4B corresponding to the runs in Figure 4A. Here, without any PLL patches, a PLL-PEG brush adsorbs virtually no fibrinogen. As the PLL-patch content of the brushy surface is increased, the fibrinogen adsorption also increases. For small numbers of PLL patches, the fibrinogen kinetic traces rise slowly and become level. With greater numbers of PLL patches (on the order of 0.12 mg/m^2 or 3500 patches/μm^2), fibrinogen adsorption is initially rapid, with a rate approaching that seen on a saturated PLL layer in the inset. After some time, however, the fibrinogen adsorption slows.

The inset of Figure 4B emphasizes the extensive adsorption of fibrinogen on vast areas of a surface made cationic by the adsorption of a saturated PLL layer. Here the saturated fibrinogen coverage, approaching 5 mg/m^2, exceeds the coverage of fibrinogen on surfaces containing as much as 4000 PLL chains/μm^2.

In Figure 5B,C, fibrinogen adsorption on the patchy brush surface is summarized in terms of the ultimate fibrinogen coverage and also in terms of its initial binding rate. The two representations are necessitated by the protracted fibrinogen binding kinetics at long times on the more densely patchy surfaces in Figure 4B. Regardless of the choice of metric for fibrinogen adsorption, an important point becomes clear: There is a threshold in the density of patches that must be achieved before fibrinogen will adsorb to the surface. Beyond this threshold, fibrinogen coverage and its binding rate increase with increasing cationic patch density, though the coverage can be quite low. Conversely, when the PLL patch density is on the order of 4000/μm^2, fibrinogen adsorption approaches (within a factor of 2 or so) the levels seen on purely PLL surfaces (inset of Figure 4B).

The diagonal line in Figure 5B marks fibrinogen adsorption levels that would correspond to one per cationic patch.

Discussion

The threshold in patch density for fibrinogen adsorption in Figure 5B,C occurs near 1500 patches/μm^2, which we believe to be greater (within the significance of experimental error) than for the onset of reduced brush coverage at 900 PLL patches/μm^2 in Figure 5A. Therefore, we conclude that the effect of the PLL patches on PLL-PEG backfilling is different from their effect on fibrinogen adsorption. Indeed, if the two thresholds were to occur at the same PLL patch density, then one would simply conclude that PLL patches at the base of the brush were entirely shielded by the PEG corona and any reduction in the PEG corona (reduced backfilling) caused by the PLL patches would immediately lead to fibrinogen adsorption. Instead, Figure 5B,C shows that even with some overall reduction in the PEG brush relative to full saturation, resistance to fibrinogen persists. The subsequent limited fibrinogen adsorption just above the threshold motivates a consideration of the PLL patches and brush structure near the patches, rather than a discussion of the overall or average properties of the brush.

First, it is worth noting that the presence of a threshold patch density for fibrinogen adsorption implies that individual isolated PLL patches are unable to capture and hold fibrinogen molecules. Instead, two or more patches are involved in fibrinogen capture. It may be the case that at the lowest patch densities, below 900/μm^2, the patches are simply buried within the brush and completely shielded by the corona. Indeed, it is interesting to consider whether a 9 nm patch can be entirely shielded by the particular PEG brushes in this study. When the PLL-PEG coverage is near the saturation level of 1.1 mg/m^2, we expect a PEG chain extension or brush height of 9 nm, as calculated in the Supporting Information. Near a patch, some of these stretched PEG tethers will spill sideways and obstruct the patch (Figure 2C), reducing its accessible area and fibrinogen binding energy. Indeed, with a brush height of 9 nm and a similar length scale for the sideways extension of PEG tethers over PLL patches, it becomes a possibility that PLL patches are completely hidden from approaching proteins. (Patch accessibility will also depend on the conditions for protein exposure, for instance, the relative exposure and brush relaxation times.)

In the dilute patch limit above, widely spaced PLL patches are sufficiently hidden in a saturated PLL-PEG brush that they cannot individually bind fibrinogen. At higher patch loadings, fibrinogen likely adsorbs by bridging multiple patches. At some point, however, the binding energy per patch will increase relative to the dilute patch limit because the brush structure around the patches becomes compromised. Bridging and further "revealing" of patches are mechanisms that must ultimately act in concert to facilitate protein capture.

Two distinct mechanisms for brush compromise at elevated PLL patch loadings will act together in statistical proportion. First, above 900 PLL patches/μm^2, PLL-PEG coverage is reduced because of the net reduction in surface area available for further copolymer adsorption. (Here, the PLL patches are still far enough apart, 33 nm on average, that the likelihood of PLL exclusion between neighboring pairs of patches is small.) The reduced PLL-PEG adsorption gives rise to a smaller extension of the PEG chains and a less robust brush. This in turn compromises the ability of the PEG brush to obscure isolated PLL patches, increasing the binding energy and probability for fibrinogen adsorption. A second mechanism for brush compromise will become important at higher PLL patch loadings when two adsorbed patches lie sufficiently close that PLL-PEG chains might be excluded between them. (Whether this actually occurs depends on whether the cationic backbone of the adsorbing chain can sufficiently uncoil to fill the narrow region of the surface between two patches. If backbone chain deformation on adsorption occurs appreciably, then this surface exclusion mechanism will not occur.) Such exclusion might occur only when the patch centers are smaller than roughly 15 nm in separation. With a Poisson distribution for the arrangement of random patches on a surface, one finds that only 5% of the patches could exclude a brush between pairs when there are 900 patches/μm^2. At the threshold for fibrinogen adsorption, 1500 PLL patches/μm^2, 11% of the patches will be paired so as potentially to exclude a brush and be an effectively larger fibrinogen patch.

We discuss a final point about fibrinogen adsorption onto the surfaces, in light of the small adhesive patches and the relatively large fibrinogen size: $47 \times 4.5 \times 4.5$ nm^3. It is not obvious that fibrinogen would adhere to as few as two to three small adhesive regions, as we argue above. Our interpretation of Figure 5B,C is, however, consistent with previous reports of fibrinogen binding in small exposed areas between previously adsorbed proteins near saturation coverage.[34] Indeed, we previously demonstrated that fibrinogen could adhere tightly with an effective footprint of 120 nm^2 or less, even approaching the footprint of lysozyme (12.6 nm^2) on the same surfaces.[8] Adhesive regions the same size as the protein itself are not a prerequisite for protein binding. In light of fibrinogen's ability to bind small regions of a surface and from our inferences about the structure of the patchy brush, we conclude that completely obscuring patches in a brush is not necessary to avoid protein adsorption. Wide separation of partially obscured elements will avoid protein adsorption if the binding energy per patch is sufficiently weak. The compromise of the brush at increased patch density further favors protein adsorption.

Conclusions

This work has demonstrated the creation of patchy brush surfaces that are useful for protein manipulation. The study also illustrates general principles for the structure and performance of polymer brushes whose tethered chains are modestly stretched normal to the substrate.

Although proteins such as fibrinogen generally adsorb to most surface chemistries, including the cationic polymer layers in the current study, protein capture becomes impossible when adhesive elements of the same chemistry are widely spaced and sufficiently small or substantially shielded by a nonadhesive polymer brush. The PEG brushes in the current study are typical composed of "pegylated" protein-resistant biomaterials. This study emphasizes that protein resistance is maintained even when the PEG tethers form marginal brushes compared with rigorously defined brushes in the polymer physics literature. The study further demonstrates that these marginal brushes are effective at concealing a substantial number of buried adhesive moieties from proteins that are otherwise very adhesive. Ultimately, it was demonstrated that protein adhesion occurred when the adsorbing protein could make multiple surface contacts and when the local PEG tether concentration was sufficiently low that brush formation was compromised.

The observation of a threshold adhesive patch density for protein adsorption is a quantitative feature that is potentially tunable through surface design and solution conditions for the precise manipulation of protein adsorption. The tunable protein–surface contacts facilitated by patches embedded in a bioresistant brush facilitate protein immobilization; however, in future

studies, limited protein−surface contact may prove to preserve structure.

Acknowledgment. This work was supported by NSF DMR-08-05061, CBET-04-28455, and (to J.L.R.) NSF DBI 0923318. Zeta potential measurements were made on an instrument within the UMass Center for Hierarchical Manufacturing, supported by NSF CMMI-0531171.

Supporting Information Available: Demonstration of patch deposition and retention. Controlled PLL deposition to make cationic patches. TIRF experiment for the adsorption of fluorescently labeled PLL, subsequently challenged by flowing buffer, PLL-PEG, and fibrinogen. Calculation of brush height. This material is available free of charge via the Internet at http://pubs.acs.org.